The Plant Cell, Vol. 15, 1198–1211, May 2003, www.plantcell.org © 2003 American Society of Plant Biologists

# *CLAVATA1* Dominant-Negative Alleles Reveal Functional Overlap between Multiple Receptor Kinases That Regulate Meristem and Organ Development

**Anne Diévart,[a] Monica Dalal,[a] Frans E. Tax,[b] Alexzandria D. Lacey,[c] Alison Huttly,[c] Jianming Li,[a] and Steven E. Clark[a,1]**

[a] Department of Molecular, Cellular, and Developmental Biology, University of Michigan, Ann Arbor, Michigan 48109-1048
[b] Department of Molecular and Cellular Biology, University of Arizona, Tucson, Arizona 85721
[c] IACR–Long Ashton Research Station, Department of Agricultural Sciences, University of Bristol, Long Ashton, Bristol BS41 9AF, United Kingdom

**The CLAVATA1 (CLV1) receptor kinase controls stem cell number and differentiation at the Arabidopsis shoot and flower meristems. Other components of the CLV1 signaling pathway include the secreted putative ligand CLV3 and the receptor-like protein CLV2. We report evidence indicating that all intermediate and strong *clv1* alleles are dominant negative and likely interfere with the activity of unknown receptor kinase(s) that have functional overlap with CLV1. *clv1* dominant-negative alleles show major differences from dominant-negative alleles characterized to date in animal receptor kinase signaling systems, including the lack of a dominant-negative effect of kinase domain truncation and the ability of missense mutations in the extracellular domain to act in a dominant-negative manner. We analyzed chimeric receptor kinases by fusing *CLV1* and *BRASSINOSTEROID INSENSITIVE1* (*BRI1*) coding sequences and expressing these in *clv1* null backgrounds. Constructs containing the CLV1 extracellular domain and the BRI1 kinase domain were strongly dominant negative in the regulation of meristem development. Furthermore, we show that *CLV1* expressed within the pedicel can partially replace the function of the ERECTA receptor kinase. We propose the presence of multiple receptors that regulate meristem development in a functionally related manner whose interactions are driven by the extracellular domains and whose activation requires the kinase domain.**

## INTRODUCTION

The generation of aerial organs in plants is dependent on the activity of shoot and flower meristems. Shoot meristems maintain organogenesis by balancing the proliferation of a population of undifferentiated stem cells at their centers and directing appropriately positioned descendant cells toward organ formation and eventual differentiation. Some mutants have been found to disrupt this balance, altering the structure and function of shoot and flower meristems. Mutations in the Arabidopsis *CLAVATA* loci (*CLV1*, *CLV2*, and *CLV3*) lead to ectopic accumulation of stem cells at shoot and flower meristems (Clark et al., 1993, 1995; Kayes and Clark, 1998). Enlarged *clv* meristems result in extra flower organs, club-shaped siliques, and enlarged inflorescence stems. Molecular genetic studies indicate that the primary function of the *CLV* loci is to restrict the expression domain of the stem cell–promoting factor *WUSCHEL* (*WUS*). *WUS* encodes a putative homeodomain transcription factor that has been shown to be both necessary and sufficient for stem cell identity (Laux et al., 1996; Mayer et al., 1998). The *WUS* expression domain expands in *clv* mutants, and ectopic expression of *WUS* within the meristem is sufficient to promote stem cell identity (Brand et al., 2000, 2002; Schoof et al., 2000; Lenhard et al., 2002).

*clv1* alleles vary greatly in phenotypic severity, ranging from weak alleles with only modest increases in stem cell number to strong alleles with >1000-fold more undifferentiated cells compared with the wild type (Clark et al., 1993). Mutant alleles of *clv1*, *clv2*, or *clv3* show strong correlations between shoot and flower meristem defects. Increases in flower meristem size are reflected in an increase in the number of organs per flower, especially the number of carpels, as well as in the extent of continued proliferation and organogenesis of the flower meristem beyond the initiation of the whorl-four carpels (Clark et al., 1993). Carpel number typically has been used to measure the severity of *clv* mutant defects.

The receptor-like kinases (RLKs), of which CLV1 is a member, represent one of the largest gene families in the Arabidopsis genome. One-third of the ~610 RLKs contain Leu-rich repeats (LRRs) in their extracellular domains (Shiu and Bleecker, 2001). LRRs are found in tandem repeats that each contain ~24 amino acids with conserved leucines. LRRs are present in a variety of proteins with diverse functions, from yeast to animals and plants, and many are involved in protein–protein interactions. Among the ~220 transmembrane LRR receptors in Arabidopsis, only a few have known functions. The challenge now is to identify their signaling components, ligands, and mechanisms of activation. Substantial efforts have been devoted to a

[1] To whom correspondence should be addressed. E-mail clarks@umich.edu; fax 734-647-0884
Article, publication date, and citation information can be found at www.plantcell.org/cgi/doi/10.1105/tpc.010504.

few LRR-RLKs that play critical roles in development. These include CLV1, BRASSINOSTEROID INSENSITIVE1 (BRI1), which is involved in the perception and signaling of the steroid hormone brassinolide (BL), and ERECTA (ER), which regulates organ shape (Torii et al., 1996; Clark et al., 1997; Li and Chory, 1997; He et al., 2000). The LRR-RLKs can be subdivided into subfamilies on the basis of numbers and locations of LRRs in their extracellular domains (Shiu and Bleecker, 2001). This classification puts CLV1 and ER in the same group of LRR-RLKs with 21 LRRs in their extracellular domains. On the other hand, BRI1 belongs to a separate subfamily because it possesses 25 LRRs and an island of 70 amino acids between the 20th and 21st LRRs. This island is proposed to mediate BRI1 binding to BR (Li and Chory, 1997; He et al., 2000). The ligand for the ER receptor remains unknown.

The CLV1 pathway, although still poorly understood, is one of the best characterized receptor kinase pathways in plants. The other two *CLV* genes, *CLV2* and *CLV3*, have been cloned and encode components of the same signal transduction pathway that regulates stem cell behavior. CLV2 belongs to the receptor-like protein family and contains LRR motifs in its predicted extracellular domain but no intracellular kinase domain (Jeong et al., 1999). *CLV3* encodes a small polypeptide that has been shown to be secreted (Fletcher et al., 1999; Rojo et al., 2002). The *CLV1*, *CLV2*, and *CLV3* genes function in the same pathway, the formation of active CLV1 complexes requires CLV3, *CLV3* overexpression phenotypes require CLV1 and CLV2, and CLV3 is secreted from cells adjacent to those expressing *CLV1*—all suggesting that CLV3 acts as the ligand for CLV1 (Clark et al., 1995, 1997; Fletcher et al., 1999; Trotochaud et al., 1999; Brand et al., 2000; Rojo et al., 2002).

Since the first description of the *clv* mutant phenotype more than a decade ago, 10 different alleles of *clv1* have been discovered and described (Leyser and Furner, 1992; Medford et al., 1992; Clark et al., 1993, 1997; Pogany et al., 1998). They exhibit phenotypes ranging from weak (*clv1-6* and *clv1-7*) to intermediate (*clv1-1*, *clv1-2*, and *clv1-9*) to strong (*clv1-4*, *clv1-8*, and *clv1-10*). All of the alleles that exhibit strong or intermediate phenotypes contain missense mutations within the LRR or the kinase coding sequences (Clark et al., 1997). Interestingly, the weakest alleles, *clv1-6* and *clv1-7*, contain a frameshift and a nonsense mutation, respectively, near the beginning of the kinase domain that could eliminate most of the kinase domain. Although the *clv1-6* and *clv1-7* alleles suggested possible dominant-negative properties of the intermediate and strong alleles, it has not been possible to exclude a low level of readthrough or the notion that the truncated proteins performed significant signaling activity.

Here, we provide evidence that all strong and intermediate *clv1* alleles are dominant negative. We have isolated three insertional alleles that all exhibit weak phenotypes. We show that cosuppression of *clv1-1* mRNA expression partially suppresses Clv1$^-$ phenotypes and that chimeric CLV1/BRI1 receptors can act as dominant-negative proteins in meristem development. We also show that CLV1 expressed within pedicels can regulate their development. Finally, we propose that multiple receptor kinases with functional overlap act within the meristem and perhaps in other organs as well.

## RESULTS

### Characterization of Three T-DNA Insertions in the *CLV1* Locus

Despite the sequencing of over 10 *clv1* alleles, no clear null alleles have been identified (Clark et al., 1997). All of the *clv1* alleles that exhibit a strong or intermediate phenotype contain missense mutations within the coding sequence (Figures 1A and 1C). Even *clv1-10*, which was identified as an intragenic enhancer of *clv1-1*, contains a second missense mutation in the LRR domain (see Methods). The only alleles with nonsense or frameshift mutations are *clv1-6* and *clv1-7*, which were isolated in pollen mutagenic screens for additional *clv1* alleles (Clark et al., 1993). However, the lesions in *clv1-6* and *clv1-7* both occur after the transmembrane domain, leaving the possibility that the proteins these alleles encode are expressed, located to the plasma membrane, and capable of signaling (Figures 1A and 1C). Precedence for this idea comes from the disease resistance receptor kinase Xa-21, which is capable of functioning without a kinase domain (Wang et al., 1998).

To determine the null phenotype for *CLV1*, we identified one Ds transposable element (DsE) and two T-DNA insertion *clv1* alleles. We named these three new alleles *clv1-11*, *clv1-12*, and *clv1-13* (see Methods). *clv1-12* was isolated in the Wassilewskija-2 (Ws-2) background and contains a T-DNA insertion in the third LRR. *clv1-13* was isolated in the Ws-2 background, and a T-DNA insertion was identified between kinase conserved motifs IV and V. *clv1-11* was isolated in the Landsberg *erecta* (L*er*) background and contains a DsE insertion in the sixth LRR (Figure 1A). The location of each insertion was determined by PCR amplification of flanking regions followed by sequencing of the PCR products (data not shown). Reverse transcriptase (RT)–PCR was performed on wild-type, *clv1-11*, *clv1-12*, and *clv1-13* RNA samples to verify that these were null alleles. We detected no accumulation of transcripts corresponding to sequences downstream of the *clv1-11* and *clv1-12* insertions (Figure 1B).

*clv1* mutant plants accumulate stem cells at their shoot and flower meristems, leading to enlarged meristems and additional floral organs. Although wild-type plants develop exclusively two carpels in whorl four of the flower, flowers of the strongest *clv1* mutants develop up to eight carpels, and a fifth whorl of ectopic organs develops inside the gynoecium generated by the whorl four of carpels (Clark et al., 1993). The number of carpels formed per flower and the extent of growth of the ectopic whorls reflect an early increase in flower meristem size and are sensitive indicators of *clv1* mutant severity (Clark et al., 1993, 1995). We compared *clv1-11* in the L*er* background with *clv1-6*, *clv1-1*, and *clv1-4*, our reference weak, intermediate, and strong alleles, respectively. Both the number of carpels per flower and the size of the fifth whorl were analyzed. The phenotype of *clv1-11* was less severe than that of *clv1-1* and was comparable to those of the weak alleles *clv1-6* and *clv1-7* (Figures 1D and 1E) (Clark et al., 1993). Note the club shape of the siliques of the intermediate *clv1-1* and strong *clv1-4* alleles compared with those of the weak allele *clv1-11* (Figure 1E). *clv1-12* and *clv1-13* displayed similarly weak phenotypes (see below). Thus, the *clv1* null phenotype is weak, suggest-

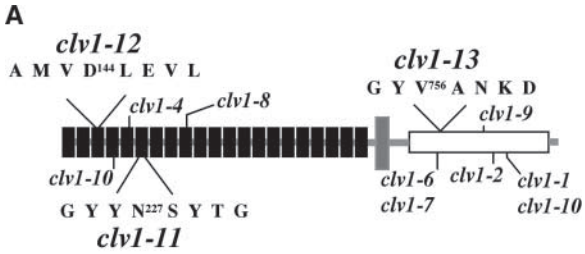


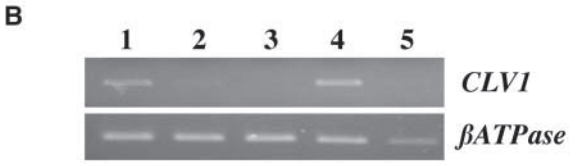


C

| Alleles | Phenotypes | Mutations | Domain |
|---|---|---|---|
| *clv1-1* | intermediate | G856D | kinase VIII |
| *clv1-2* | intermediate | G881E | kinase IX |
| *clv1-4* | strong | G201E | LRR 5 |
| *clv1-6* | weak | R751* | kinase IV |
| *clv1-7* | weak | R751K[a] | kinase IV |
| *clv1-8* | strong | D295N | LRR 9 |
| *clv1-9* | intermediate | A839V | kinase VII |
| *clv1-10* | strong | G177E and G856D | LRR 4 and kinase VIII |

[a] following sequence: TSWLRSEQGYESPSL*

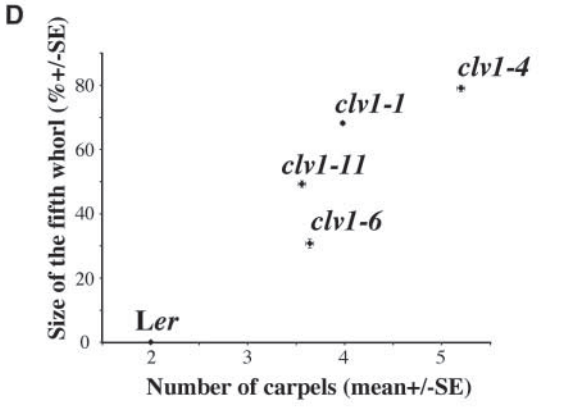


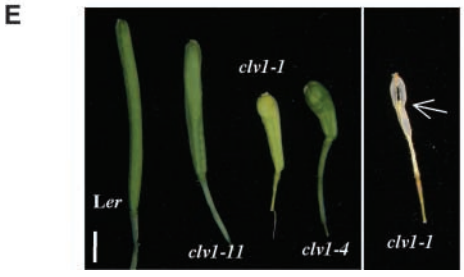


**Figure 1.** Alleles of *clv1*.

**(A)** Scheme of known alleles of *clv1* and locations of the DsE insertion (*clv1-11*) and the T-DNA insertions (*clv1-12* and *clv1-13*) of three novel null alleles of *clv1*. The amino acid sequences surrounding the integration sites are indicated. The LRRs (black boxes), transmembrane domain (gray box), and kinase domains (white box) are represented.

**(B)** Ethidium bromide agarose gels from the RT-PCR performed on Col (lane 1), *clv1-12* (lane 2), *clv1-13* (lane 3), L*er* (lane 4), and *clv1-11* (lane 5) samples. mRNA isolated from inflorescences was analyzed by RT-PCR to monitor the transcript accumulation of *CLV1*. Each PCR amplification of the cDNA was generated in parallel with specific primers for *CLV1* (top gel) and control (*βATPase*; bottom gel). RT-PCR products from Col and L*er* plants were examined as controls.

**(C)** For each allele, the phenotypic severity, the amino acid mutated, and the domain affected are indicated.

**(D)** Relative size of the fifth whorl compared with the number of carpels in *clv1-1*, *clv1-6*, *clv1-11*, *clv1-4*, and L*er*. Ten flowers from at least 20 primary inflorescences of 30-day-old plants were scored for the number of carpels (means ± SE). The size of the silique represents the length between the attachment site for the sepals, petals, and stamens and the top of the gynoecium. The same references were used for the measurement of fifth-whorl length. The measured size of the fifth whorl is represented as a percentage of total silique length. The vertical and horizontal bars represent standard errors for the relative fifth-whorl size and the number of carpels, respectively. Note that there is no fifth whorl in L*er* and that the number of carpels does not vary from two, so the standard error is 0.

**(E)** Comparison of siliques from L*er* plants. The shape of the siliques from L*er*, *clv1-11*, *clv1-1*, and *clv1-4* varies with the severity of the Clv1$^-$ phenotype. Note the club shape of the intermediate *clv1-1* and strong *clv1-4* alleles compared with the weak *clv1-11* silique shape. At right is shown a dry *clv1-1* silique revealing the fifth whorl of organ growing inside the gynoecium and representing ~70% of the size of the silique. Bar = 2 mm.

ing that strong and intermediate *clv1* alleles may be dominant negative.

### Generation of CLV1-BRI1 Chimeric Receptors

To determine the requirement for individual CLV1 domains in regulating meristem development, we generated various chimeric receptors (Figure 2). The coding sequences for portions of CLV1 were fused to those for the steroid receptor kinase BRI1 under the control of the *ER* promoter. *ER* encodes a receptor kinase that regulates organ shape and that is expressed broadly within the meristems and developing organ primordia (Yokoyama et al., 1998). We chose the *ER* regulatory sequences to drive expression for several reasons. First, *ER* expression appears to entirely encompass the *CLV1* expression domain (Yokoyama et al., 1998). Second, despite using extended upstream and downstream sequences, we failed to isolate *CLV1* regulatory sequences that can rescue *clv1* mutants or mimic *CLV1* expression (data not shown). Third, ER encodes a receptor kinase, so we would not be driving expression of the chimeric receptors at unusually high levels. The *ER*:*CLV1* construct provided close to complete rescue of the Clv1$^-$ phenotype when transformed into *clv1-1* plants (Figure 3A). The mean number of carpels per flower in *clv1-1 ER*:*CLV1* plants is only slightly higher than that of *clv1-1*/+ heterozygous plants (Clark et al., 1996), suggesting that the *ER* promoter likely drives ex-

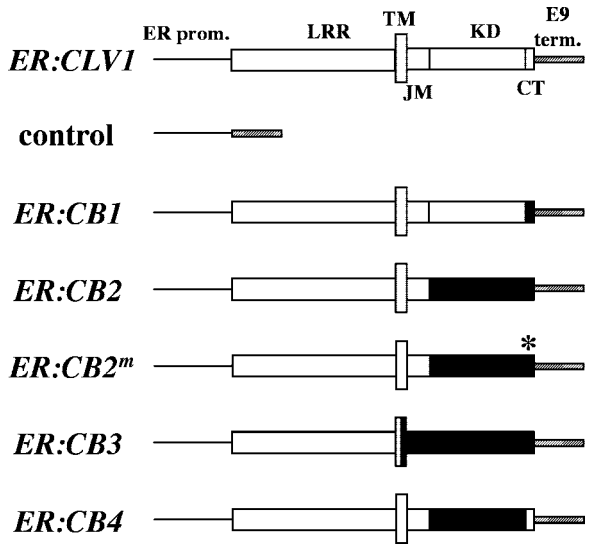


**Figure 2.** Schemes (Not to Scale) of the *CLV1* cDNA (*ER*:*CLV1*), *ER*:*CB1*, *ER*:*CB2*, *ER*:*CB2*$^m$, *ER*:*CB3*, and *ER*:*CB4* Chimeric Receptor Kinase, and Control Transgenes.

The CLV1 and BRI1 protein structures are shown as white and black boxes, respectively. The junction between CLV1 and BRI1 in each chimeric construct did not alter the amino acid sequence of CLV1 or BRI1. The mutation introduced in the BRI1 kinase domain to produce the *ER*:*CB2*$^m$ transgene (asterisk) is located in domain IX and is the same as the *bri1-101* mutation, which results in a loss of kinase activity (Friedrichsen et al., 2000). These constructs are driven by the *ERECTA* promoter (black line; 1678 bp of sequence upstream of *ER*), contain the E9 terminator (hatched box), and are cloned into pCB302 (Xiang et al., 1999) (see Methods). CT, C-terminal tail; ER prom., *ER* promoter; JM, juxtamembrane domain; KD, kinase domain; E9 term., E9 terminator; TM, transmembrane domain.

pression within the meristem close to the level of the endogenous *CLV1* gene.

The coding sequences for CLV1 and BRI1 were divided into the extracellular LRR domain (Figure 2, LRR), the transmembrane domain (Figure 2, TM), the juxtamembrane domain (between the transmembrane domain and the first conserved kinase domain sequences; Figure 2, JM), the conserved kinase domain (Figure 2, KD), and the C-terminal tail lacking specific kinase domain motifs (Figure 2, CT). The *ER*:*CB2*$^m$ construct included the Glu-to-Lys mutation in domain IX of the kinase domain, which is found in the loss-of-function *bri1-101* mutation (Li and Chory, 1997) (Figure 2).

### *clv1-1* Cosuppression Rescues the Clv1$^-$ Phenotype

Direct evidence that *clv1-1* is dominant negative came unexpectedly from experiments with these CLV1/BRI1 chimeric receptors. The *ER*:*CLV1*, *ER*:*CB1*, *ER*:*CB2*, *ER*:*CB2*$^m$, *ER*:*CB3*, and *ER*:*CB4* constructs were transformed into *clv1-1* plants and tested for the ability to rescue the Clv1$^-$ phenotype. As described above, the number of carpels per flower and the extent of whorl-five growth were used as measures of meristem size and CLV1 function.

When *ER*:*CB2*, *ER*:*CB2*$^m$, *ER*:*CB3*, and *ER*:*CB4* were transformed into *clv1-1*, we observed that 15 to 50% of the T1 plants for each construct exhibited partial suppression of the Clv1$^-$ phenotype (Table 1). When analyzed in detail in subsequent generations, these lines exhibited a clear reduction in mean carpel number and fifth-whorl growth (Figure 3A). The sizes of the shoot apical meristems of the affected transgenic lines also were suppressed compared with the fasciated *clv1-1* shoot meristems (Figure 3B).

We suspected that the Clv1$^-$ phenotypic suppression was attributable to cosuppression of the endogenous *clv1-1* transcript for two reasons. First, all of the lines gave rise to the same phenotype, regardless of the specific construct transformed (e.g., the kinase-active *ER*:*CB2* and the kinase-inactive *ER*:*CB2*$^m$ chimeric constructs provided similar *clv1-1* suppression). Second, the phenotypically suppressed transgenic *clv1-1* plants were very similar in phenotype to the *clv1* null mutants.

To determine the role of *clv1-1* cosuppression in Clv1$^-$ phenotype suppression, the expression of *clv1-1* and each transgene was analyzed by RT-PCR in phenotypically suppressed transgenic lines (Figures 4A and 4B). In every phenotypically suppressed line analyzed, we observed one of two expression patterns. (1) For most suppressed *clv1-1 ER*:*CLV1* lines, we detected significant *ER*:*CLV1* transgene expression. (2) For two suppressed *clv1-1 ER*:*CLV1* lines and all suppressed *clv1-1 ER*:*CB2*, *ER*:*CB2*$^m$, and *ER*:*CB3* lines tested, the expression of the endogenous *clv1-1* gene was reduced compared with that in controls (Figures 4A and 4B).

These data suggested that cosuppression of endogenous *clv1-1* gene expression could lead to Clv1$^-$ phenotypic suppression. Consistent with this finding, we observed a correlation between Clv1$^-$ phenotype suppression and a weak/intermediate Bri1$^-$ phenotype, suggesting cosuppression of both the *clv1-1* and *BRI1* genes in these lines (Table 1). In subsequent generations, some plants lost *BRI1* cosuppression with no effect on Clv1$^-$ phenotypic suppression (data not shown). Moreover, a portion of the T1 transgenic plants exhibited only *clv1-1* or *BRI1* cosuppression. Together, these data suggest that the Clv1$^-$ phenotype suppression was not attributable to a reduction in *BRI1* activity.

### Dominant-Negative Chimeric Receptors

Because the dominant-negative nature of the endogenous *clv1-1* allele complicated the analysis of chimeric receptor function, we chose to transform all chimeric constructs into the *clv1-11* null background. At least 30 primary transformants were obtained for each construct, and 5 to 14 lines were examined in detail in the T2 generation. The goal was to assess chimeric receptor function by monitoring suppression of the Clv1$^-$ phenotype; however, we observed that many of the constructs resulted in an enhancement of the Clv1$^-$ phenotype.

The two constructs that did provide Clv1$^-$ rescue were *ER*:*CLV1* and *ER*:*CB1*. *clv1-11 ER*:*CLV1* plants were nearly wild type in meristem phenotype, again suggesting that the *ER* regulatory sequences drive expression close to the level of the

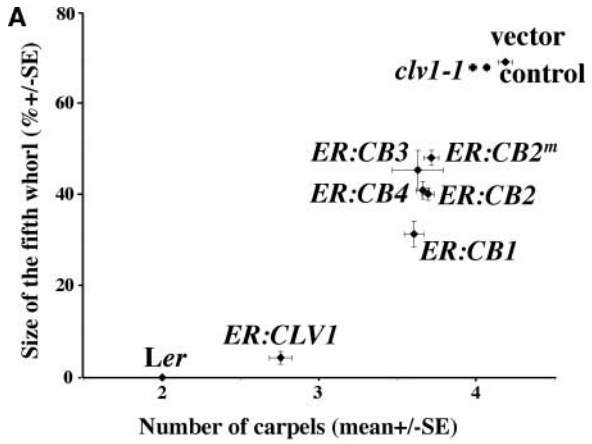


| | No. of plants analyzed | No. of lines analyzed | No. of siliques counted | No. of siliques dissected |
|---|---|---|---|---|
| Ler | 61 | N.A. | 610 | 610 |
| *clv1-1* | 22 | N.A. | 306 | 177 |
| control | 54 | 8 | 802 | 120 |
| vector | 12 | 5 | 120 | 120 |
| *ER:CLV1* | 88 | 11 | 1661 | 95 |
| *ER:CB1* | 28 | 13 | 280 | 280 |
| *ER:CB2* | 75 | 16 | 1161 | 200 |
| *ER:CB2$^m$* | 22 | 12 | 220 | 220 |
| *ER:CB3* | 44 | 12 | 440 | 300 |
| *ER:CB4* | 47 | 17 | 470 | 460 |

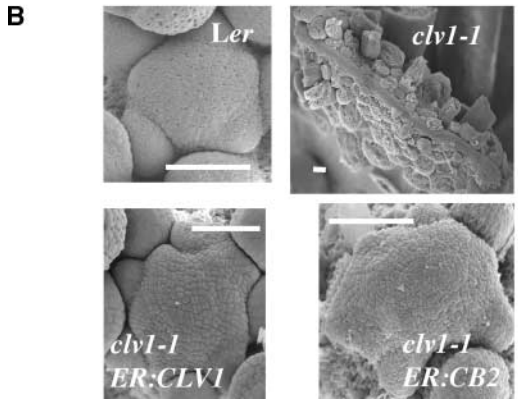


**Figure 3.** CLV1/BRI1 (CB) Chimeric Receptors Rescue the *clv1-1* Mutant Phenotype.

**(A)** Relative size of the fifth whorl compared with the number of carpels in L*er*, *clv1-1*, and *clv1-1* transformed with the *ER*:*CLV1*, *ER*:*CB1*, *ER*:*CB2*, *ER*:*CB2$^m$*, *ER*:*CB3*, *ER*:*CB4*, empty vector, and control transgenes. The number of independent transgenic lines and the number of T3 plants analyzed are shown in the table at bottom. Between 10 and 20 fully expanded siliques of 30-day-old plants were counted for the number of carpels and dissected for the size of the fifth whorl before desiccation. The size of the fifth whorl growing inside the gynoecium was measured and compared with the size of the silique to give its relative size (% ± SE) (cf. Figure 1D). The vertical and horizontal bars represent standard errors for the fifth whorl size and the number of carpels, respectively.

**(B)** Scanning electron micrographs of the shoot apical meristems of 30-day-old plants. Note that the shape of the meristems of *clv1-1 ER*:*CLV1* and *clv1-1 ER*:*CB2* transgenic plants is closer to that of L*er* than to the fasciated *clv1-1* meristem. Bars = 500 μm.

endogenous *CLV1* gene (Figures 5A and 5B). The *ER*:*CB1* construct, which provided significantly poorer rescue of *clv1-1* compared with the *ER*:*CLV1* construct (Figure 3A), provided nearly complete rescue of *clv1-11* (Figures 5A and 5B). This finding suggests that the C-terminal domain of CLV1 contains no motifs specific for CLV1 signaling.

The *ER*:*CB2*, *ER*:*CB2$^m$*, *ER*:*CB3*, and *ER*:*CB4* transgenes enhanced the *clv1-11* mutant phenotype. This enhancement included all aspects of the Clv1$^-$ phenotype: mean carpel number, extent of fifth-whorl growth, overall silique morphology, and size of the shoot apical meristem (Figures 5A and 5B). Both the wild-type and mutant versions of the BRI1 kinase domains in *ER*:*CB2* and *ER*:*CB2$^m$*, respectively, were equally effective in enhancing the Clv1$^-$ phenotype. The *ER*:*CB3* construct contained just the extracellular domain of CLV1 and retained dominant-negative effects. The *ER*:*CB4* construct, in which only the kinase domain of CLV1 was replaced by the BRI1 kinase domain, enhanced the *clv1-11* phenotype as well, suggesting that neither the juxtamembrane domain nor the C-terminal tail domain is involved in the induction of the dominant-negative effect. Each dominant-negative transgene gave rise to a similar level of Clv1$^-$ phenotype enhancement, suggesting similar target(s) and mechanisms of action. Thus, constructs containing a CLV1 extracellular domain and a BRI1 kinase domain exhibited a dominant-negative effect.

We did not observe the induction of any phenotypes outside of the meristem with any of the chimeric receptors with the exception of Bri1$^-$ phenotypes. As we observed for these transgenes in the *clv1-1* background, the chimeric constructs induced cosuppression of *BRI1* in ~20% of the lines analyzed. These plants did not show *clv1-11* suppression and were comparable phenotypically to *clv1-11* (data not shown).

### Precise *CLV1* Expression Is Not Essential for Its Function

*CLV1* normally is expressed specifically within the internal cell layers of the shoot meristem, predominantly the L3 layer (Clark et al., 1997; Fletcher et al., 1999; Trotochaud et al., 1999). *CLV3* is expressed in overlying, minimally overlapping cells in the L1, L2, and topmost L3 layers (Fletcher et al., 1999). Remarkably, driving *CLV1* expression under the control of the *ER* regulatory elements, which drive endogenous and transgene expression in all layers of the shoot meristem (Yokoyama et al., 1998), in *clv1-1* and *clv1-11* plants had no impact on meristem development beyond rescuing the Clv1$^-$ phenotype. When *ER*:*CLV1* was transformed into wild-type plants, no effect on shoot or flower meristem development was observed (data not shown).

**Table 1.** *clv1-1* and *BRI1* Cosuppression in Transgenic *clv1-1* Plants

| Plant Lines | No. of T1 Plants | No. of T1 Transgenic Plants with *Bri1*$^-$ Phenotype[a] | No. of Lines with *Clv1*$^-$ Suppression[b] | No. of Lines with Only *Bri1*$^-$ Suppression[a] | No. of Lines with Only *Clv1*$^-$ Suppression[b] |
|---|---|---|---|---|---|
| *clv1-1* | NA[c] | 0/22 | 0/22 | 0/22 | 0/22 |
| Control | 145 | 0/145 | 0/145 | 0/145 | 0/145 |
| Vector | 30 | 0/30 | 0/30 | 0/30 | 0/30 |
| *ER*:*CLV1* | 47 | 0/47 | 24/47 (51%) | 0/47 | 24/47 (51%) |
| *ER*:*CB1* | 36 | 2/36 (5.5%) | 16/36 (44%) | 0/36 | 14/36 (39%) |
| *ER*:*CB2* | 150 | 33/150 (22%) | 36/150 (24%) | 4/150 (2.66%) | 7/150 (4.66%) |
| *ER*:*CB2*$^m$ | 73 | 21/73 (28.7%) | 20/73 (27.4%) | 4/73 (5.48%) | 3/73 (4.1%) |
| *ER*:*CB3* | 67 | 10/67 (14.9%) | 10/67 (14.9%) | 0/67 | 0/67 |
| *ER*:*CB4* | 27 | 4/27 (14.8%) | 14/27 (51.8%) | 1/27 (3.7%) | 11/27 (40.7%) |

[a] Number of dwarf-looking plants.
[b] Number of plants with fewer than four carpels.
[c] Not applicable.

### CLV1 Can Function Outside of the Meristem

The elongation of internodes and pedicels is important in determining the overall aerial structure of plants. Each flower meristem gives rise to flower organs that are separated from the inflorescence stem by a pedicel. The pedicel elongates with the development of floral organs. Mutant screens for altered inflorescence branching patterns have revealed *ER* (Torii et al., 1996; Yokoyama et al., 1998; Lease et al., 2001a) and other genes (Lease et al., 2001b; Venglat et al., 2002). The commonly used Arabidopsis L*er* ecotype harbors the *er* mutation, resulting in an altered inflorescence branching pattern caused by a reduction in the length of internodes and pedicels, the growth of clustered flowers at the apex of the inflorescence, and shorter, wider, and blunt-tipped siliques. A precise analysis of stems and pedicels of *er* mutant plants indicated that the short stem/pedicel phenotype is attributable mainly to a decrease in cell number (Yokoyama et al., 1998).

We initially observed that the size of siliques and pedicels of the *clv1-1 er* and *clv1-11 er* plants transformed with the *ER*:*CLV1* construct was increased compared with that in *clv1-1 er* and *clv1-11 er*, respectively (data not shown). Because the *ER*:*CLV1* construct also suppressed the meristem defects of *clv1-1* and *clv1-11* mutants, we could not exclude the possibility that the increase in pedicel and silique size in *clv1-1 er ER*:*CLV1* and *clv1-11 er ER*:*CLV1* transgenic plants was the indirect consequence of a restoration of normal meristem function. To eliminate transgene-induced changes in meristem size, the *ER*:*CLV1* construct was introduced into L*er* plants and the size of the siliques and pedicels was scored. The pedicels of L*er ER*:*CLV1* plants were 27% longer than the pedicels of L*er* plants transformed with the control construct (wild-type pedicel, 7.74 $\pm$ 0.05 mm, $n = 185$; *ER*:*CLV1* pedicel, 9.82 $\pm$ 0.03 mm, $n = 166$). Interestingly, the length of the gynoecium was not affected significantly by the *ER*:*CLV1* construct (wild-type silique, 12.96 $\pm$ 0.05 mm, $n = 185$; *ER*:*CLV1* silique, 12.42 $\pm$ 0.07 mm, $n = 166$). Thus, the expression of *CLV1* under the control of the *ER* promoter can partially rescue the pedicel but not the gynoecium phenotypes of *er* plants, indicating that CLV1 can function outside of the meristem.

### Ecotype Genetic Variation Affects Phenotypes of *clv1* Mutants

During backcrosses of two of the *clv1* null alleles from the Ws-2 background (*clv1-12* and *clv1-13*) into L*er*, we detected a significant effect of ecotype background on the severity of Clv1$^-$ phenotypes (Table 2). Note that in the analysis described below, we detected a significant frequency of a "valveless" phenotype among some of the genotypes tested, as indicated in Table 2. This phenotype was first described in detail for *clv2* mutants, which often develop replum tissue in the place of carpels, such that the flowers can develop one or even zero carpels (Kayes and Clark, 1998). In flowers with the valveless phenotype, carpel number is no longer an accurate reflection of flower meristem defects. Thus, we also calculated the number of carpels per flower from mutant plants using only those flowers that did not exhibit a valveless phenotype. These measurements are described below.

*clv1-12* displayed a mean carpel number of 2.57 $\pm$ 0.05 per flower in the Ws-2 *ER* background and a mean carpel number of 3.12 $\pm$ 0.04 in the first backcross into the L*er* background (Table 2), revealing a highly significant effect of the L*er* background on the *clv1-12* phenotype (Table 3). Similarly, the mean carpel number of *clv1-13* mutants increased from 2.64 $\pm$ 0.05 to 3.28 $\pm$ 0.04 in the same backcross (Table 2), which again is highly significant based on Student's *t* test (Table 3).

To determine if this enhancement of *clv1* null phenotypes was the result of ecotype variation, due to the *er* mutation, and/or specific for *clv1*, we analyzed *clv1* and *clv3* mutants in a number of backcrosses (Tables 2 and 3). *clv1-12* crossed to the *er-123* allele within the same Ws-2 background displayed a lesser, but statistically significant, effect compared with crosses into L*er*. This finding indicates that there is both a specific but minor effect from the *er* mutation and a larger effect of the Landsberg background. We observed a significant phenotypic enhancement when crossing *clv1-12* in the Ws-2 *ER* background to the Col *ER* background, again revealing an ecotype effect (Tables 2 and 3). However, there was no detectable difference between crossing *clv1-12* to the Col *ER* or the Col *er-106* background, suggesting that the specific effect of *er* is minor and/or masked

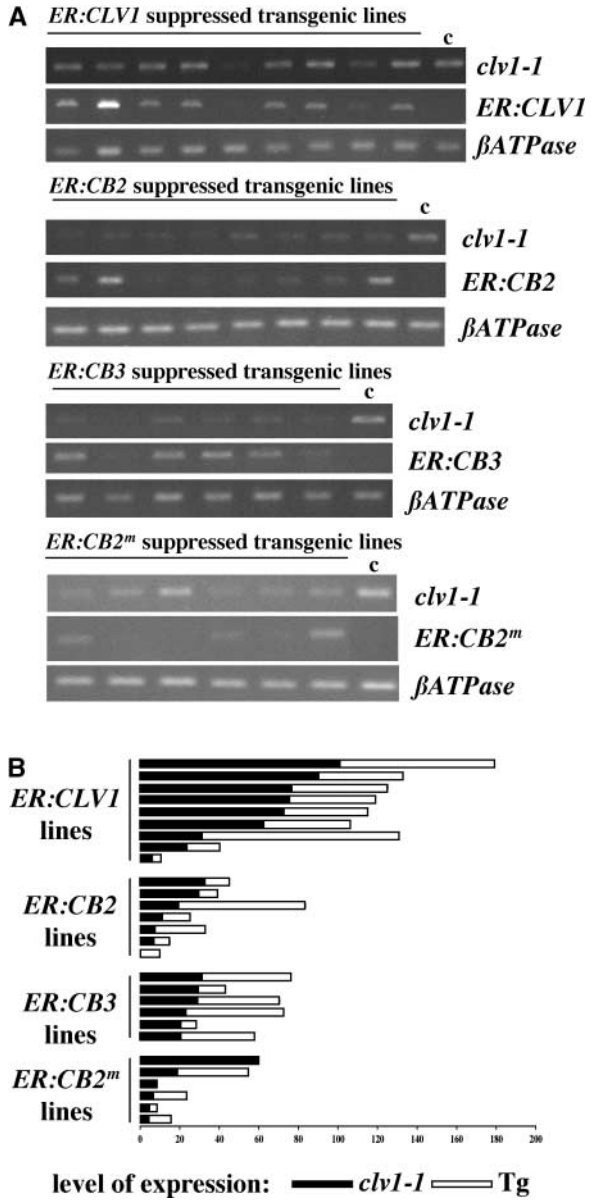


**Figure 4.** *clv1-1* Is Dominant Negative.

**(A)** Ethidium bromide agarose gels from RT-PCR performed on individual suppressed transgenic lines (see Methods). T1 inflorescence RNA samples for *clv1-1 ER*:*CLV1*, *clv1-1 ER*:*CB2*, *clv1-1 ER*:*CB3*, and *clv1-1 ER*:*CB2*$^m$ transgenic plants were analyzed by RT-PCR to monitor transcript accumulation of the endogenous *clv1-1* and transgene mRNA. Each lane corresponds to one transgenic line. RT-PCR products from *clv1-1* nontransgenic plants, *clv1-1* control transgenic plants, and no RNA were examined as controls (c) in all cases. Each PCR amplification of the cDNA was generated in parallel with specific primers for *clv1-1* (top gel), the appropriate transgene (middle gel), and the control (*βATPase*; bottom gel). Top panel, *clv1-1 ER*:*CLV1* transgenic lines; second panel, *clv1-1 ER*:*CB2*; third panel, *clv1-1 ER*:*CB3*; fourth panel, *clv1-1 ER*:*CB2*$^m$.

**(B)** Quantification and normalization of the RT-PCR agarose gel data (see Methods). Black boxes indicate *clv1-1* expression, and white boxes indicate transgene (Tg) expression.

by the Col background. *clv1-13* displayed results similar to *clv1-12* (Tables 2 and 3).

*clv1-4*, which is in an uncharacterized ecotype listed by McKelvie (1962) as either Estland or Limbaugh, exhibited effects of both *er* or a linked factor and ecotype backgrounds. *clv1-4 er-123* and *clv1-4 ER* plants analyzed from a segregating mixed ecotype population revealed a minor, but statistically significant, enhancement of the Clv1$^-$ phenotype in plants homozygous for *er* (Tables 2 and 3). A much stronger Clv1$^-$ enhancement was observed in *clv1-4* crossed to the L*er* background (Tables 2 and 3).

*clv3* mutants, on the other hand, displayed different effects of ecotype backgrounds and the *er* mutation. *clv3-2* and *clv3-8* are presumed null alleles that have phenotypes similar to that of *clv1-4* (Clark et al., 1995). We observed no significant differences between the *clv3-2* allele from the L*er* background and the *clv3-8* allele from an unknown *ER* background (Tables 2 and 3). The weak *clv3-3* allele has a phenotype similar to that of *clv1* null alleles (Fletcher et al., 1999). We observed a significant effect of crossing *clv3-3 ER* from the Ws-2 background to L*er*. However, the phenotype of *clv3-3* crossed to L*er* was suppressed compared with the phenotype of *clv3-3* in the Ws-2 *ER* background, which is the opposite of our observation for *clv1* null alleles. Thus, ecotypes to a major degree, and the *er* mutation to a minor degree, have a specific effect on the phenotype of *clv1* mutants. Pursuing the genes responsible for the ecotype differences could prove useful in identifying additional factors that interact with CLV1 and/or other redundant receptor kinases.

## DISCUSSION

Previous models of CLV1 signaling did not explain differences in the observed effects of *clv1* alleles. Specifically, the observation that alleles with absent kinase domains (*clv1-6* and *clv1-7*) exhibited weaker phenotypes than those with missense mutations within the LRR and/or kinase domains could not be explained easily. Alleles of *clv2* and *clv3* displayed no such disparity between lesion and phenotypic effect (Clark et al., 1995; Kayes and Clark, 1998; Fletcher et al., 1999; Jeong et al., 1999). This work provides several lines of evidence suggesting that the stronger *clv1* alleles are dominant negative and likely interfere with additional receptor kinase(s) within the meristems (Figure 6). By assessing the dominant-negative effects of CLV1/BRI1 chimeric receptors, we provide evidence defining receptor interactions and show that CLV1 and BRI1 kinase domains are not interchangeable. Furthermore, our results indicate that CLV1 can act outside of the meristem to regulate pedicel length in the absence of ER function. Finally, ectopic expression of *CLV1* within the meristem does not disrupt normal meristem development.

### Unknown Receptor Kinase(s) May Share Functions with CLV1

Several lines of evidence support the existence of an additional receptor kinase(s) that has functional overlap with CLV1 (Figure

A

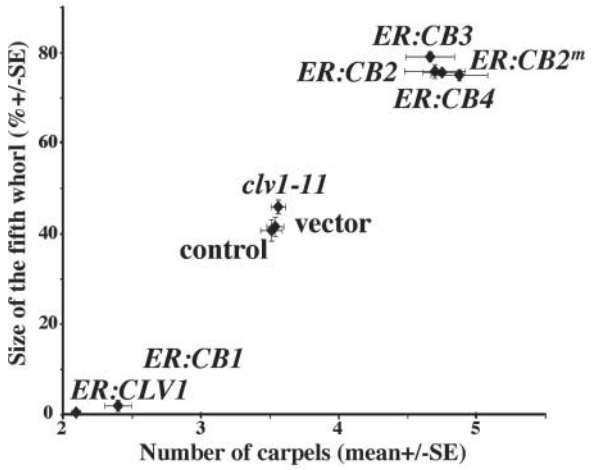


| | No. of plants analyzed | No. of lines analyzed | No. of siliques counted and dissected |
|---|---|---|---|
| *clv1-11* | 25 | N.A. | 250 |
| control | 29 | 5 | 290 |
| vector | 30 | 8 | 300 |
| *ER:CLV1* | 18 | 7 | 180 |
| *ER:CB1* | 19 | 8 | 190 |
| *ER:CB2* | 21 | 8 | 210 |
| *ER:CB2m* | 22 | 10 | 220 |
| *ER:CB3* | 17 | 9 | 170 |
| *ER:CB4* | 22 | 14 | 220 |

B

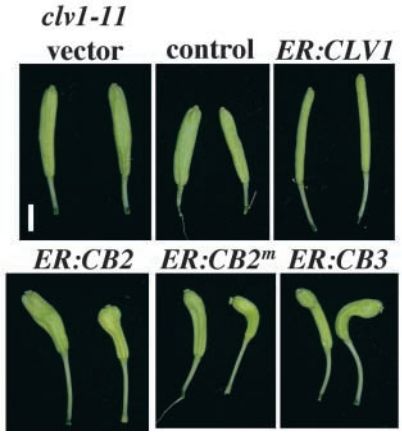


**Figure 5.** The Chimeric Receptors CB2, CB2$^m$, CB3, and CB4 Are Dominant Negative.

**(A)** The relative size of the fifth whorl compared with the number of carpels in *clv1-11* and *clv1-11* transformed with *ER:CLV1*, *ER:CB1*, *ER:CB2*, *ER:CB2$^m$*, *ER:CB3*, *ER:CB4*, empty vector, and control transgenes. The number of independent transgenic lines and the number of T3 plants analyzed are shown in the table at bottom. Ten fully expanded siliques of 30-day-old plants were counted for the number of carpels and dissected for the size of the fifth whorl before desiccation. The vertical and horizontal bars represent standard errors for the fifth whorl size and the number of carpels, respectively. Note that the almost complete rescue of the *clv1-11* phenotype is observed for *ER:CLV1* and *ER:CB1*. On the other hand, the chimeric receptors *ER:CB2*, *ER:CB2$^m$*, *ER:CB3*, and *ER:CB4* enhance the phenotypes of *clv1-11* plants.

**(B)** Comparison of the silique shapes of *clv1-11* plants transformed with *ER:CLV1*, *ER:CB2*, *ER:CB2$^m$*, *ER:CB3*, empty vector, and control transgenes. Note that the shape of the *ER:CLV1* siliques is close to that of wild-type siliques and that the siliques of *ER:CB2*, *ER:CB2$^m$*, and *ER:CB3* transgenic plants are club shaped, reflecting a more severe phenotype than that seen in the *clv1-11* and control lines. Bar = 2 mm.

6). The first such indication came from analyses of three new null alleles of *clv1*, each of which displayed weak phenotypes comparable to those of *clv1-6* and *clv1-7* mutants. This finding suggested that all of the intermediate and strong mutant *clv1* alleles are dominant negative. Consistent with this hypothesis, cosuppression of the expression of the intermediate *clv1-1* allele in transgenic plants partially rescued the mutant *clv1-1* phenotype, such that the cosuppressed plants appeared phenotypically similar to *clv1* null mutants.

Many different types of proteins could be inactivated by clv1 dominant-negative protein isoforms, including ligands, other receptor kinases, and cytoplasmic signaling factors. Previous genetic analyses of *clv3* mutants are most consistent with a receptor kinase(s) being the target of mutant clv1 interference (Figure 6). The strongest dominant-negative alleles of *clv1* approach the phenotype of *clv3* null alleles, and *clv3* null alleles are epistatic to weak, intermediate, and strong *clv1* alleles (Clark et al., 1993, 1995). Thus, CLV3 retains some function in *clv1* mutants, especially in *clv1* null mutants. Because CLV3 is secreted and required to activate CLV1 (Trotochaud et al., 1999; Rojo et al., 2002), CLV3 must activate another target in *clv1* null mutants, presumably a receptor kinase. Furthermore, the hypothesis that the clv1 dominant-negative isoforms sequester the putative CLV3 ligand is not consistent with studies on a likely feedback loop between WUS and CLV3 (Brand et al., 2000; Schoof et al., 2000; Lenhard et al., 2002). The net result of this loop is to increase *CLV3* expression in mutant plants in which CLV signaling is diminished. Indeed, *CLV3* expression as detected by RNA in situ hybridization is increased in *clv1* mutant backgrounds (Brand et al., 2000). Thus, CLV3 is unlikely to be rate limiting in the *clv1* dominant-negative backgrounds.

If an additional receptor kinase functions in overlap with CLV1, why has this receptor not been identified in genetic screens? One possible explanation is that the unknown receptor has a somewhat lesser role in CLV3 signaling, such that mutant alleles might not exhibit a phenotype. *clv1* null alleles display fairly subtle deviations from the wild type in some ecotype backgrounds, so that a receptor with lower expression levels or lesser signaling effectiveness compared with CLV1 might not display any significant phenotype. Part of the reason for this might lie in the CLV3/WUS feedback loop. A second possible explanation is that the unknown receptor also might function in additional developmental pathways, such that mutants would display pleiotropic phenotypes. Finally, the unknown receptor might be represented by more than one gene, such that inacti-

**Table 2.** Ecotype Background and *er* Modify *clv1* and *clv3* Phenotypes

| Plant | Ecotype[a] | No. of Siliques Analyzed | No. of Carpels per Flower (mean ± SE) | Valveless Siliques (%) | No. of Carpels Excluding Valveless Siliques (mean ± SE)[b] | Relative Size of the Fifth Whorl (% ± SE) |
|---|---|---|---|---|---|---|
| *clv1-4 ER* | Unk.[c]/Ws-2 | 330 | 3.58 ± 0.04 | 51 | 4.15 ± 0.02 | >80 |
| *clv1-4 er123* | Unk.[c]/Ws-2 | 250 | 3.71 ± 0.06 | 54 | 4.39 ± 0.04 | >80 |
| *clv1-4 er* | Unk.[c]/*Ler* | 100 | 5.2 ± 0.09 | 15 | 5.35 ± 0.08 | >80 |
| *clv1-12 ER* | Ws-2 | 260 | 2.57 ± 0.05 | 0 | 2.57 ± 0.05 | 0 |
| *clv1-12 er123* | Ws-2 | 160 | 2.83 ± 0.06 | 0 | 2.83 ± 0.06 | 1.25 ± 0.62 |
| *clv1-12 ER* | Ws-2/Col | 240 | 2.77 ± 0.05 | 0 | 2.77 ± 0.05 | 1.93 ± 0.54 |
| *clv1-12 er106* | Ws-2/Col | 210 | 2.81 ± 0.05 | 0 | 2.81 ± 0.05 | 0 |
| *clv1-12 er* | Ws-2/*Ler* | 280 | 3.12 ± 0.04 | 0 | 3.12 ± 0.04 | 12.13 ± 1.15 |
| *clv1-13 ER* | Ws-2 | 260 | 2.64 ± 0.05 | 0 | 2.64 ± 0.05 | 0 |
| *clv1-13 ER* | Ws-2/Col | 200 | 2.71 ± 0.05 | 0 | 2.71 ± 0.05 | 0.25 ± 0.20 |
| *clv1-13 er106* | Ws-2/Col | 170 | 2.66 ± 0.06 | 0 | 2.66 ± 0.06 | 1.23 ± 0.51 |
| *clv1-13 er* | Ws-2/*Ler* | 270 | 3.28 ± 0.04 | 0 | 3.28 ± 0.04 | 6.25 ± 0.97 |
| *clv3-2 er* | *Ler* | 230 | 5.29 ± 0.05 | 0 | 5.29 ± 0.05 | >80 |
| *clv3-8 ER* | Unk.[d] | 117 | 4.16 ± 0.11 | 50 | 5.10 ± 0.08 | >80 |
| *clv3-3 er* | Ws-2/*Ler* | 285 | 2.57 ± 0.04 | 0 | 2.57 ± 0.04 | 0 |
| *clv3-3 ER* | Ws-2 | 274 | 2.78 ± 0.05 | 0 | 2.78 ± 0.05 | 0 |

[a] Populations with two ecotypes indicated refer to a segregating F2 population of a cross between the two ecotypes.
[b] Mean number of carpels per flower excluding flowers exhibiting the valveless phenotype.
[c] Unknown, Estland or Limbaugh.
[d] Unknown.

vation of any one gene would not exhibit a phenotype. Note that most of our genetic screens have been performed in the *clv1-1* mutant background, in which the activity of any receptors with functional overlap would be expected to be reduced as a result of the dominant-negative character of this allele. Ideally, genetic screens should be performed in the *clv1* null mutant background, in which the activity of these hypothetical receptors would be most important phenotypically.

### Potential Mechanisms by Which Dominant-Negative *clv1* Alleles Act

Most of the *clv1* alleles identified to date are dominant negative. The severity of the phenotypes of these mutant proteins varies depending on the location of the lesion within the CLV1 protein. The mutations that give an intermediate phenotype are clustered in the activation loop of the kinase domain. The mutations that give a strong phenotype are found in the fourth, fifth, and ninth LRRs in the predicted extracellular domain (Figure 6).

We were unable to find any example in the literature of dominant-negative mutations within the extracellular domains of animal receptor kinases. Missense mutations in the ligand binding domain of the receptor-Tyr kinase torso and deletion of the Toll extracellular domain are gain-of-function mutations (Schneider et al., 1991; Li et al., 2002b). The dominant-negative mutations in *CLV1* are localized in LRRs four, five, and nine and are situated in or close to the predicted β-strand of the respective LRRs. Interestingly, these mutants exhibit a stronger phenotype than the dominant-negative mutations located in the cytoplasmic domain. Their phenotypes approach that of *clv3* null mutants. The fact that the phenotype is stronger with the LRR-located mutations than with the mutations in the cytoplasmic domain suggests that the blockage of the signaling pathway by the mutations in the cytoplasmic domain is not complete (Figure 6).

For lesions in the kinase domain, we noted several differences and similarities when comparing *clv1* alleles with dominant-negative mutations in animals. Deletion of all or part of the cytoplasmic domain of the receptor-Tyr kinase epidermal growth factor receptors or other receptor-Tyr kinases results in dominant-negative mutations (Kashles et al., 1991; Chen et al., 1993; Prager et al., 1994; Guichard et al., 2002). The two *CLV1* alleles that mimic this kind of mutation, *clv1-6* and *clv1-7*, exhibit a weak phenotype similar to that of null alleles. Several explanations for this difference can be suggested. The truncated clv1-6 and clv1-7 receptors could be unstable at the plasma membrane or mislocalized. If stable at the plasma membrane, the clv1-6 and clv1-7 mutant proteins would appear unable to interfere with receptors present in the meristem that have functional overlap.

Most of the dominant-negative mutations in protein kinases (TGF-β receptor, MEKK1, Alk6, IGF-1R, and IRAK-4) or in receptor-Tyr kinases (IGF-1R and IRAK-4) in animals are clustered at the ATP binding site of the kinase domain, corresponding to domain II of CLV1 (Kong et al., 1994; Sanchez et al., 1994; Zou and Niswander, 1996; Kalebic et al., 1998; Li et al., 2002a). It is of interest that no *clv1* alleles have been identified that contain mutations within key catalytic residues of the kinase domain, suggesting that some catalytic activity may be required within the full-length CLV1 for receptor interaction and, hence, dominant-negative properties. We have noted that when expressed as kinase domains in *Escherichia coli*, clv1-1, clv1-2, and clv1-9 retain some autophosphorylation activity (data not shown). Interestingly, the mutations in *clv1-1*, *clv1-2*, and *clv1-9* lie within or close to the activation loop in the kinase domain (Torii and Clark, 2000). Some mutations in animals are

comparable to these: the $EGFR^{DN3}$ mutation is located in domain VIb, and the *bmpr2* mutation is located between domains VIb and VII (Zou and Niswander, 1996; Guichard et al., 2002; Rudarakanchana et al., 2002). Studies on *bmpr2* showed that this dominant-negative mutant is not expressed at the plasma membrane but instead is retained in the endoplasmic reticulum (Rudarakanchana et al., 2002).

The phenotypes observed in *clv1-1* plants suggest that the mutant protein is able to interfere with the signaling of other receptors with functional overlap. This interference could occur by clv1 proteins interacting directly with the other receptors and blocking their function (Figure 6). Consistent with the idea of a direct interaction between receptors, the *clv1-1* allele was described previously as incompletely dominant (Clark et al., 1995, 1996). Moreover, the hypothesis that dominant-negative clv1 isoforms interfere with the function of other receptors is consistent with the extent of $Clv1^-$ rescue when *ER*:*CLV1* and *ER*:*CB1* were transformed into *clv1-1* and *clv1-11* plants. Both of these constructs are nearly able to completely rescue the *clv1-11* null phenotype, suggesting that in the absence of dominant-negative protein isoforms, both wild-type CLV1 and CB1 are effective transducers of CLV3 signal. However, in the presence of *clv1-1*, both CLV1 and CB1 are significantly less effective at signaling, as measured by the partial $Clv1^-$ rescue each provides. The phenotype of *clv1-1 ER*:*CLV1* plants is similar to that of *clv1-1*/+ plants, consistent with *ER* elements driving expression within the meristem at levels similar to those in the endogenous *CLV1* gene. *clv1-1 ER*:*CB1* plants are nearly as severe as *clv1* null alleles, indicating that CB1 function is particularly sensitive to clv1-1 interference.

We previously examined clv1 protein accumulation in various *clv1* mutant plants (Trotochaud et al., 1999). These studies revealed that clv1 dominant-negative isoforms accumulate within the meristem; however, we were unable to conclude that these proteins accumulate normally, because the proportion of meristem cells per sample was affected dramatically by the $Clv1^-$ phenotype. The various clv1 isoforms were identified as components of protein complexes, some of them similar to CLV1 complexes observed in wild-type plants, although the extracellular domain isoforms were found in a novel complex of an apparently monomeric size. However, it is difficult to draw clear conclusions about the mechanism of clv1 dominant-negative action from this approach for several reasons. First, most of the components of the complexes are unknown. Second, it is not certain that complexes from different genotypes of approximately the same size are in fact the same protein complexes. Third, interactions responsible for clv1 dominant-negative properties might not be stable under our isolation methods and thus might not be represented in our analysis. The identification of other receptor(s) that have functional overlap with CLV1 would be critical for using complex formation to assess the mechanism of dominant-negative clv1 function and potential receptor interactions.

### Dominant-Negative Chimeric Receptors

Although the chimeric CB1 receptor kinase was functional, especially in a *clv1* null background, the proteins encoded by the chimeric constructs *ER*:*CB2*, *ER*:$CB2^m$, *ER*:*CB3*, and *ER*:*CB4* appear to act as dominant-negative proteins. These constructs transformed into *clv1-1* and *clv1-11* plants enhanced the mutant phenotype, with transgenic plants displaying an increased number of carpels per flower and an enlarged fifth whorl compared with *clv1-1* and *clv1-11* plants. Thus, expression of the extracellular domain of CLV1 with a heterologous kinase domain in transgenic plants was able to block receptor signaling within the meristem in a dominant manner.

One important aspect of the chimeric receptors is that they did not require overexpression to achieve their dominant-negative character. Expression of wild-type *CLV1* under the control of the *ER* regulatory elements in *clv1-1* and *clv1-11* plants is consistent with *ER*-driven expression being close to, but less than, the expression level of the endogenous *CLV1* gene. The same *ER* regulatory sequences driving *ER*:*CB2*, *ER*:$CB2^m$, *ER*:*CB3*, and *ER*:*CB4* expression in *clv1-11* plants give rise to phenotypes stronger than those seen in *clv1-1*, *clv1-2*, and *clv1-9* plants. Indeed, the phenotype of these chimeric receptors is similar to that of the strong *clv1-4* allele.

Each of the receptors *ER*:*CB2*, *ER*:$CB2^m$, *ER*:*CB3*, and *ER*:*CB4* resulted in nearly identical phenotypes when transformed into *clv1-11*. This finding suggests a common mechanism for these receptors in interfering with signaling within the meristem. This indicates that kinase activity is not required for interference, because the putative kinase-active CB2 and ki-

**Table 3.** Statistical Tests of Phenotypic Variation

| Reference Plants | Compared with | Student's *t* Test P Value | Significantly Different? |
|---|---|---|---|
| *clv1-12 ER* (Ws-2) | *clv1-12 er123* (Ws-2) | 0.00081 | Yes |
| | *clv1-12 er* (Ws-2/L*er*) | $4.13\ E^{-16}$ | Yes |
| | *clv1-12 ER* (Ws-2/Col) | 0.00163 | Yes |
| *clv1-12 ER* (Ws-2/Col) | *clv1-12 er106* (Ws-2/Col) | 0.59704 | No |
| *clv1-13 ER* (Ws-2/Col) | *clv1-13 er106* (Ws-2/Col) | 0.58964 | No |
| *clv1-4 ER* (Unk.[a]/Ws-2) | *clv1-4 er123* (Unk.[a]/Ws-2) | $8.69\ E^{-5}$ | Yes |
| | *clv1-4 er* (Unk.[a]/L*er*) | $1.48\ E^{-39}$ | Yes |
| *clv3-3 ER* (Ws-2) | *clv3-3 er* (Ws-2/L*er*) | 0.00119 | Yes |
| *clv3-8 ER* (Unk.)[b] | *clv3-2 er* (L*er*) | 0.09590 | No |

[a] Unknown, Estland or Limbaugh.
[b] Unknown.

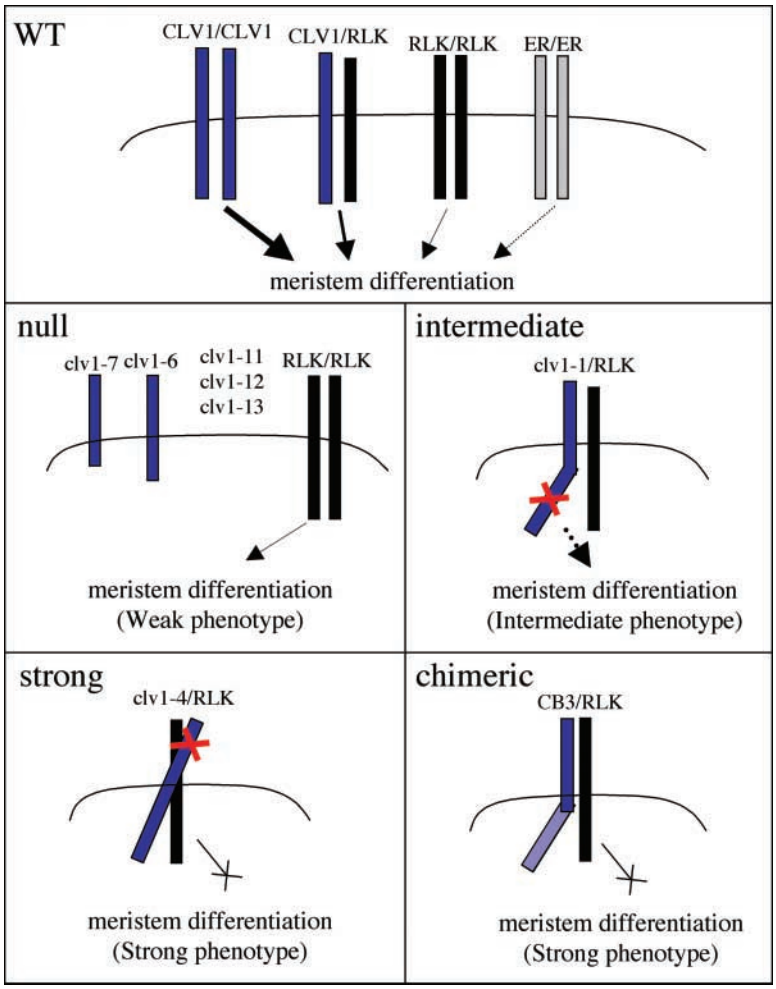


**Figure 6.** Model of Dominant-Negative Receptor Action.

A speculative model for the role of CLV1, an additional unknown receptor kinase with functional overlap (RLK), and ER in regulating meristem development. Scenarios for wild-type plants (WT), *clv1* null mutants, intermediate *clv1* mutants, strong *clv1* mutants, and the dominant-negative chimeric receptors are indicated. The model predicts receptor interactions between CLV1 and RLK, which can lead to interference with RLK function in the presence of clv1 dominant-negative isoforms and in the presence of chimeric receptors. The thickness of the arrows suggests the relative strength of signaling, and lesions in clv1 proteins are indicated with a red X.

nase-inactive $CB2^{m}$ were similar in severity. It also indicates that the key to the dominant-negative function is likely the substitution of the BRI1 kinase domain, because this feature is common to all four constructs. Thus, although the kinase domains of the plant LRR-RLKs show strong sequence similarity (the kinase domains of CLV1 and BRI1 show 63% similarity), they are not interchangeable.

### Natural Variation Affects Meristem Development

We have observed that the phenotypes of various *clv1* alleles are affected significantly by natural variation between different Arabidopsis ecotypes. In fact, in every case, crossing *clv1* alleles from one ecotype to another resulted in significant modification of the mutant phenotype. The strongest $Clv1^{-}$ phenotype enhancement was observed in crosses to the L*er* background. A significant, albeit lesser, portion of this enhancement appeared to be the consequence of the *er* mutation within this ecotype. This finding suggests some overlap in function between CLV1 and ER within the shoot meristem. The activity of these receptors clearly is not equivalent in meristem regulation, based on driving CLV1 expression under the control of the ER regulatory elements. The effect of the *er* mutation could reflect a low level of nonspecific crosstalk between the CLV1 and ER signaling pathways. In the L*er* backcrosses, we conclude that the majority of the phenotypic enhancement is the result of non-*er* factors. Furthermore, other ecotype backcrosses in which the wild-type *ER* allele was fixed also resulted in significant phenotypic variation. Importantly, in at least some cases, this variation appeared to be specific for *CLV1*. The genes responsible for this natural variation make good candidates for CLV1-interacting factors.

### Ectopic *CLV1* Expression Affects Pedicel, but Not Meristem, Development

The *ER* regulatory elements have been shown to match endogenous ER patterns and to drive expression throughout the meristem as well as in developing organ primordia (Yokoyama et al., 1998). The putative ligand for CLV1, *CLV3*, and the target of CLV1 signaling, *WUS*, both are expressed only within specific cell layers of the shoot meristem, with the exception that *WUS* also is expressed in ovule primordia (Gross-Hardt et al., 2002). Thus, it is of interest to determine if CLV1 placed in ectopic locations at the physiologically relevant levels provided by *ER* regulatory elements can exert any effect on signaling or development. Any phenotypic effect of CLV1 ectopic expression would suggest that CLV1 is capable of interacting with additional signaling systems. We observed that pedicel length was affected significantly by the *ER*:*CLV1* transgene in L*er* plants. Because pedicel length was shortened by the *er* mutation, the *ER*:*CLV1* transgene suppressed the Er$^-$ pedicel phenotype. Given the overlap in ER and CLV1 function detected within the meristem, one possible explanation for this finding is that CLV1 replaces ER function within the developing pedicels. The *ER*:*CLV1* suppression of *er* phenotypes does not extend to the Er$^-$ gynoecium phenotypes. Lease et al. (2001b) recently described *agb1*, a mutant allele of the heterotrimeric G-protein β-subunit, which exhibits phenotypes similar to those of *er*. They concluded that AGB1 may function with ER to regulate aspects of silique development but may function in parallel in other aspects of development. Thus, ER may use alternate signaling mechanisms in different tissues. This finding may explain the differential effect of CLV1 on Er$^-$ phenotypes. However, many pathways affect organ elongation, and there is no way at this time to conclude that CLV1 acts within the ER pathway in pedicels.

Surprisingly, one site where ectopic *CLV1* expression did not affect development was in the shoot meristem. Here, the location of *CLV1* expression matched well the adjacent expression of the putative ligand, CLV3, and the expression of the target, WUS, in a subdomain of CLV1 expression (Clark et al., 1997; Mayer et al., 1998; Fletcher et al., 1999). One could predict that ectopic *CLV1* expression within the L1 and L2 layers of the shoot meristem would block CLV3 signal generated in the L1 and L2 layers from reaching L3, where *WUS* normally is repressed by CLV1 action. However, we observed no such effect, suggesting either that the CLV3/WUS feedback loop overcomes any ligand sequestration by CLV1 or that the L1 and L2 layers lack the factors necessary for the presumed CLV1–CLV3 interaction.

## METHODS

### *clv1* and *clv3* Alleles

The *clv3-3* allele (line CS6421) of *Arabidopsis thaliana* was identified in ecotype Wassilewskija-2 (Ws-2) and obtained from the ABRC at Ohio State University (Columbus). *clv3-3* was backcrossed to Landsberg *erecta* (L*er*) to isolate the *clv3-3 er* double mutant. The *clv3-2* allele has been described previously (Clark et al., 1995; Fletcher et al., 1999). The *clv3-8* allele (line CS3604) was isolated by G. Redei and obtained from the ABRC. No ecotype information was available for *clv3-8*. PCR analysis of this allele revealed a chromosomal breakpoint between the 5′ end of intron 2 and the 3′ end of exon 3 (data not shown), similar to the breakpoint position in *clv3-2*. The T-DNA *clv1-12* and *clv1-13* insertion lines were identified by screening the Arabidopsis Knockout Facility α population (http://www.biotech.wisc.edu/Arabidopsis/). Products were amplified by PCR with *CLV1*-specific (5′-GTTTCCGATTCCGGCCGGGATTGAACCGGT-3′ and 5′-AACTAACCTGGGGCGATGTATCCATAAGGG-3′) and JL-202 (5′-CATTTTATAATAACGCTGCGGACATCTAC-3′; left border specific) primers and sequenced to determine the site of the T-DNA insertion. These insertions are available as lines CS3954 and CS3955 from the ABRC. These two lines, originally in the Ws-2 background, were backcrossed to L*er*, Ws-2 *er-123* (Lease et al., 2001a), and Columbia *er-106* (Lease et al., 2001a) for a comparative analysis of the effect of the mutation in both backgrounds.

The F2 population was screened for the Clv1$^-$ and Er$^-$ phenotypes and allowed to self-pollinate. Phenotypic analyses were performed on the F3 generation. The *clv1-11* line (background L*er*) was generated by crossing the enhancer trap–containing T-DNA line DsE2 (CS8047) donated to the Nottingham Stock Centre by Rob Martienssen (Cold Spring Harbor Laboratory, Cold Spring Harbor, NY) to the Ac transposase T-DNA line Ac2 (CS8044). Unlinked transposition of the Ds element was screened for in the F2 population by growing seeds on naphthalene acetamide– and kanamycin-containing plates (Sundaresan et al., 1995). Doubly resistant plants were transferred to soil and allowed to self-pollinate. Phenotypic analysis of the F3 segregating population of line *clv1-11* showed the clv1 phenotype as a recessive mutation. DNA samples were taken from two plants that displayed the mutation and one that did not, and thermal asymmetric interlaced PCR was performed. Sequencing of the bands amplified in each case revealed the same sequence with an eight-base duplication of endogenous sequence, typical of Ds insertions. The sequence indicated the insertion site within the *CLV1* gene, between nucleotides 753 and 754 of the cDNA (Figure 1), which translates to amino acids 227 and 228 of the protein. Seeds from the selfed F3 plants showing the mutation were collected, and all subsequent analysis was performed on these homozygous F4 seeds.

We had reported previously that the *clv1-10* allele, which was isolated as an intragenic enhancer of *clv1-1*, contained a second mutation within the kinase domain coding sequence (Pogany et al., 1998). Subsequent analysis could not replicate this result. Resequencing of the *CLV1* coding sequence from the *clv1-10* genome revealed instead that the *clv1-10* allele contains a second lesion within the Leu-rich repeat domain coding sequence, as indicated in Figure 1.

Seeds were sown on a 1:1:1 mix of topsoil:perlite:vermiculite and allowed to imbibe for 5 days at 4°C. Plants were grown at 22°C under ~800 foot-candles of continuous cool-white fluorescent light. The transgenic constructs were introduced into *Agrobacterium tumefaciens* strain GV3101 by the heat-shock method and transformed into *clv1-1*, *clv1-11*, or L*er* by vacuum infiltration (5 min at 25 inches of Hg) (Bechtold et al., 1993; Bechtold and Pelletier, 1998). Transgenic seedlings were selected by resistance to Basta herbicide (Hoechst Schering AgrEvo, Wilmington, DE) diluted 1:1000. The plants were sprayed 10 days after germination and then three times per week for at least 2 weeks.

### *CLV1* cDNA, *CLV1*/*BRI1*, and *CLV1*/*BRI1*$^m$ Expression Constructs

For the chimeric receptor construct *ER*:*CB2*, a FauI restriction site was inserted in the *CLV1* and *BRI1* cDNA sequences in the first kinase domain by site-directed mutagenesis. Four oligonucleotides were used: FclvFauI (5′-CGGTAAAGGCGGGGCTGGAATTGTC-3′) and RclvFauI (5′-GACAATTCCAGCCCCGCCTTTACCG-3′) for *CLV1* and FbriFauI (5′-GATTGGTTCTGGCGGGTTTGGAGATG-3′) and RbriFauI (5′-CATCTCCAAACCCGCCAGAACCAATC-3′) for *BRI1*. This FauI site was used to clone the 5′ *CLV1* fragment in frame with the 3′ *BRI1* fragment to give

the amino acid sequence 5′-LKEENIIGSGGFGD-3′. A PstI-EcoRV fragment of *CB2* was replaced by the mutated *bri1-101* fragment (XhoI site at 3340 bp mutated) in *CB2$^m$*. For the *CB3* construct, an AseI site was created in the transmembrane domains of *CLV1* cDNA and *BRI1* cDNA. Four oligonucleotides were used: AseITM_CLV1f (5′-ATCACCGGATTA-ATCCTAATCA-3′) and AseITM_CLV1r (5′-GATTAGGATTAATCCGGT-GAT-3′) for insertion of the AseI site in *CLV1* cDNA and AseITM_BRI1f (5′-ATATTTGGATTAATCCTTGTTGG-3′) and AseITM_BRI1r (5′-CCA-ACAAGGATTAATCCAAATAT-3′) for insertion of the AseI site in *BRI1* cDNA. The SpeI-AseI fragment from the *CLV1* cDNA was ligated to the AseI-EcoRV fragment from *BRI1* cDNA.

For the *CB4* construct, the kinase domain of *CB2* was used as a template for PCR amplification with the oligonucleotides FbriPstI (5′-CGG-AAGATTGCGATAGGATCAG-3′) and RClvBriXIKD (5′-GTGCACAAC-TTCCCTCATTGTCGGTCGTCTCC-3′). This first PCR amplified the kinase domain of *BRI1* until domain XI of the kinase domain and added the first nucleotides of the C-terminal tail domain of *CLV1* at the 3′ end of the sequence. A second PCR was performed on the *CLV1* cDNA cloned in pBluescript II KS+ (Stratagene) with the oligonucleotides FBriClvXIKD (5′-GGAGACGACCGACAATGAGGGAAGTTGTGCAC-3′) and the T3 primer. This second PCR amplified the C-terminal tail domain of *CLV1* with a few nucleotides belonging to domain XI of the *BRI1* kinase domain at the 5′ end of the sequence. A third PCR was performed using as a template the two fragments mentioned above with the oligonucleotides FbriPstI and T3. This fragment was digested with PstI-EcoRV and ligated in the PstI-EcoRV–digested *CB2* construct to replace the C-terminal tail domain of *BRI1* with the *CLV1* C-terminal tail domain. This fragment was sequenced after cloning.

For the *CB1* construct, the same strategy was used. The first PCR amplification was performed on the *CLV1* cDNA with the primers KSQ.1 (5′-CCGCCACCGTCACATAG-3′) and RevBriClvXIKD (5′-GGCCATGAC-TTGTACCATCGTAGGCCTTGC-3′). A second PCR was performed on the *BRI1* cDNA cloned into pBluescript II KS+ (Stratagene) with the oligonucleotides ForBriClvXIKD (5′-GCAAGGCCTACGATGGTACAAGTC-ATGGCC-3′) and T7. These two fragments were used as templates in a third PCR with primers KSQ.1 and T7. The SpeI-NsiI fragment from the *CLV1* cDNA was ligated to a NsiI-EcoRV fragment from this third PCR, generating a chimeric kinase domain in which the C-terminal tail domain of *CLV1* was replaced with the C-terminal tail domain of *BRI1*. As mentioned above, the construct was sequenced after cloning. The fragment, including the *ER* promoter (−1678 bp), the *CLV1* cDNA or chimeric constructs, and the E9 terminator, was subcloned into the pCB302 vector (Xiang et al., 1999). Fragments including only the *ER* promoter and the E9 terminator inserted into the pCB302 vector and the pCB302 empty vector were used as controls.

### Scanning Electron Microscopy Analysis

Inflorescence tips of 15- or 30-day-old plants were fixed in 4% glutaraldehyde and 25 mM $NaPO_4$ overnight at 4°C. Tissues were washed in 25 mM $NaPO_4$ and incubated for several days in 1% osmium tetroxide and 25 mM $NaPO_4$ at 4°C. Samples then were dehydrated sequentially through an ethanol series. Samples were dried with a critical point drier with liquid $CO_2$, dissected to remove obstructive organs and expose the shoot apical meristem, coated with gold, and observed with a scanning electron microscope (S3200N; Hitachi, Tokyo, Japan). Images were collected digitally.

### RNA Extraction and Reverse Transcriptase–PCR

Total RNA was isolated from 100 mg of inflorescences from approximately 30-day-old plants using the Trizol reagent (Life Technologies/Gibco BRL). One microgram of total RNA was reverse transcribed from an oligo($dT_{15}$) primer in a 25-μL reverse transcription reaction as recommended by the manufacturer (*Moloney murine leukemia virus* reverse transcriptase; Promega). One microliter of the first-strand cDNA reaction was used as a template for PCR amplification with specific oligonucleotides for *CLV1* (forward, 5′-CCGCCACCGTCACATAG-3′ or 5′-CGG-CGTTGTTCTCACCGTCA-3′ [upstream of the *CLV1* intron as a control for genomic DNA contamination]; reverse, 5′-ATGATCACCACATTT-CGCATC-3′ or 5′-CCAACAGGTTTCTTCCCAGCT-3′) and *CLV1/BRI1* (forward, 5′-CGGCGTTGTTCTCACCGTCA-3′; reverse, 5′-CTGATC-CTATCGCAATCTTCCG-3′). As an internal control, primers for the Arabidopsis *βATPase* genes were used. The PCR products were loaded on ethidium bromide–stained agarose gels. Each band was quantified with the Gel Doc 2000 Gel Documentation System (Bio-Rad) using Quantity One software and normalized to the controls. First, the background of the no-DNA PCR sample was removed for the *clv1* and transgene bands. Then, the values were adjusted on the loading controls (*βATPase*). The values obtained for *clv1-1* were normalized to the *clv1-1* controls, which were assigned the value of 100. For the *ER*:*CLV1*, *ER*:*CB2*, *ER*:*CB2$^m$*, and *ER*:*CB3* transgenes, the highest *ER*:*CLV1*-expressing line was used to normalize the values of the other lines.

Upon request, all novel materials described in this article will be made available in a timely manner for noncommercial research purposes.

## ACKNOWLEDGMENTS

We thank Joshua Stomel for determining the correct sequence of the *clv1-10* allele, Brody DeYoung for the sequence of the *clv1-7* allele, Keiko Torii for isolating the *ER* promoter, Sang-Kee Song for generating the *clv3-3 er* double mutants, and Erik Colegrove for assistance in planting. This work was supported by National Institutes of Health Grant 1R01GM62962-01A1 to (S.E.C.). A.D. was supported in part by Organogenesis Postdoctoral Fellowship (University of Michigan, Ann Arbor). Isolation of *clv1-12* and *clv1-13* insertion alleles was supported by the National Science Foundation Grant DBI-9975808 to (F.E.X.).

Received January 13, 2003; accepted February 25, 2003.

## REFERENCES

**Bechtold, N., Ellis, J., and Pelletier, G.** (1993). In planta *Agrobacterium*-mediated gene transfer by infiltration of adult *Arabidopsis thaliana* plants. C. R. Acad. Sci. Paris **316,** 1194–1199.

**Bechtold, N., and Pelletier, G.** (1998). In planta *Agrobacterium*-mediated transformation of adult *Arabidopsis thaliana* plants by vacuum infiltration. Methods Mol. Biol. **82,** 259–266.

**Brand, U., Fletcher, J.C., Hobe, M., Meyerowitz, E.M., and Simon, R.** (2000). Dependence of stem cell fate in Arabidopsis on a feedback loop regulated by CLV3 activity. Science **289,** 617–619.

**Brand, U., Grunewald, M., Hobe, M., and Simon, R.** (2002). Regulation of CLV3 expression by two homeobox genes in Arabidopsis. Plant Physiol. **129,** 565–575.

**Chen, R.H., Ebner, R., and Derynck, R.** (1993). Inactivation of the type II receptor reveals two receptor pathways for the diverse TGF-beta activities. Science **260,** 1335–1338.

**Clark, S.E., Jacobsen, S.E., Levin, J.Z., and Meyerowitz, E.M.** (1996). The CLAVATA and SHOOT MERISTEMLESS loci competitively regulate meristem activity in Arabidopsis. Development **122,** 1567–1575.

**Clark, S.E., Running, M.P., and Meyerowitz, E.M.** (1993). CLAVATA1, a regulator of meristem and flower development in Arabidopsis. Development **119,** 397–418.

**Clark, S.E., Running, M.P., and Meyerowitz, E.M.** (1995). *CLAVATA3* is a specific regulator of shoot and floral meristem development affecting the same processes as *CLAVATA1*. Development **121,** 2057–2067.

**Clark, S.E., Williams, R.W., and Meyerowitz, E.M.** (1997). The CLAVATA1 gene encodes a putative receptor kinase that controls shoot and floral meristem size in Arabidopsis. Cell **89,** 575–585.

**Fletcher, J.C., Brand, U., Running, M.P., Simon, R., and Meyerowitz, E.M.** (1999). Signaling of cell fate decisions by CLAVATA3 in Arabidopsis shoot meristems. Science **283,** 1911–1914.

**Friedrichsen, D.M., Joazeiro, C.A., Li, J., Hunter, T., and Chory, J.** (2000). Brassinosteroid-insensitive-1 is a ubiquitously expressed leucine-rich repeat receptor serine/threonine kinase. Plant Physiol. **123,** 1247–1256.

**Gross-Hardt, R., Lenhard, M., and Laux, T.** (2002). WUSCHEL signaling functions in interregional communication during Arabidopsis ovule development. Genes Dev. **16,** 1129–1138.

**Guichard, A., Srinivasan, S., Zimm, G., and Bier, E.** (2002). A screen for dominant mutations applied to components in the Drosophila EGF-R pathway. Proc. Natl. Acad. Sci. USA **99,** 3752–3757.

**He, Z., Wang, Z.Y., Li, J., Zhu, Q., Lamb, C., Ronald, P., and Chory, J.** (2000). Perception of brassinosteroids by the extracellular domain of the receptor kinase BRI1. Science **288,** 2360–2363.

**Jeong, S., Trotochaud, A.E., and Clark, S.E.** (1999). The Arabidopsis CLAVATA2 gene encodes a receptor-like protein required for the stability of the CLAVATA1 receptor-like kinase. Plant Cell **11,** 1925–1934.

**Kalebic, T., Blakesley, V., Slade, C., Plasschaert, S., Leroith, D., and Helman, L.J.** (1998). Expression of a kinase-deficient IGF-I-R suppresses tumorigenicity of rhabdomyosarcoma cells constitutively expressing a wild type IGF-I-R. Int. J. Cancer **76,** 223–227.

**Kashles, O., Yarden, Y., Fischer, R., Ullrich, A., and Schlessinger, J.** (1991). A dominant negative mutation suppresses the function of normal epidermal growth factor receptors by heterodimerization. Mol. Cell. Biol. **11,** 1454–1463.

**Kayes, J.M., and Clark, S.E.** (1998). CLAVATA2, a regulator of meristem and organ development in Arabidopsis. Development **125,** 3843–3851.

**Kong, G., Penn, R., and Benovic, J.L.** (1994). A beta-adrenergic receptor kinase dominant negative mutant attenuates desensitization of the beta 2-adrenergic receptor. J. Biol. Chem. **269,** 13084–13087.

**Laux, T., Mayer, K.F., Berger, J., and Jurgens, G.** (1996). The WUSCHEL gene is required for shoot and floral meristem integrity in Arabidopsis. Development **122,** 87–96.

**Lease, K.A., Lau, N.Y., Schuster, R.A., Torii, K.U., and Walker, J.C.** (2001a). Receptor serine/threonine protein kinases in signalling: Analysis of the erecta receptor-like kinase of *Arabidopsis thaliana*. New Phytol. **151,** 133–143.

**Lease, K.A., Wen, J., Li, J., Doke, J.T., Liscum, E., and Walker, J.C.** (2001b). A mutant Arabidopsis heterotrimeric G-protein β subunit affects leaf, flower, and fruit development. Plant Cell **13,** 2631–2641.

**Lenhard, M., Jurgens, G., and Laux, T.** (2002). The WUSCHEL and SHOOTMERISTEMLESS genes fulfill complementary roles in Arabidopsis shoot meristem regulation. Development **129,** 3195–3206.

**Leyser, H.M.O., and Furner, I.J.** (1992). Characterizations of three shoot apical meristem mutants of *Arabidopsis thaliana*. Development **116,** 397–403.

**Li, J., and Chory, J.** (1997). A putative leucine-rich repeat receptor kinase involved in brassinosteroid signal transduction. Cell **90,** 929–938.

**Li, S., Strelow, A., Fontana, E.J., and Wesche, H.** (2002a). IRAK-4: A novel member of the IRAK family with the properties of an IRAK-kinase. Proc. Natl. Acad. Sci. USA **99,** 5567–5572.

**Li, W.X., Agaisse, H., Mathey-Prevot, B., and Perrimon, N.** (2002b). Differential requirement for STAT by gain-of-function and wild-type receptor tyrosine kinase Torso in Drosophila. Development **129,** 4241–4248.

**Mayer, K.F., Schoof, H., Haecker, A., Lenhard, M., Jurgens, G., and Laux, T.** (1998). Role of WUSCHEL in regulating stem cell fate in the Arabidopsis shoot meristem. Cell **95,** 805–815.

**McKelvie, A.D.** (1962). A list of mutant genes in *Arabidopsis thaliana*. Radiat. Bot. **1,** 233–241.

**Medford, J.I., Behringer, F.J., Callos, J.D., and Feldmann, K.A.** (1992). Normal and abnormal development in the *Arabidopsis* vegetative shoot apex. Plant Cell **4,** 631–643.

**Pogany, J.A., Simon, E.J., Katzman, R.B., de Guzman, B.M., Yu, L.P., Trotochaud, A.E., and Clark, S.E.** (1998). Identifying novel regulators of shoot meristem development. J. Plant Res. **111,** 307–313.

**Prager, D., Li, H.L., Asa, S., and Melmed, S.** (1994). Dominant negative inhibition of tumorigenesis in vivo by human insulin-like growth factor I receptor mutant. Proc. Natl. Acad. Sci. USA **91,** 2181–2185.

**Rojo, E., Sharma, V.K., Kovaleva, V., Raikhel, N.V., and Fletcher, J.C.** (2002). CLV3 is localized to the extracellular space, where it activates the Arabidopsis CLAVATA stem cell signaling pathway. Plant Cell **14,** 969–977.

**Rudarakanchana, N., Flanagan, J.A., Chen, H., Upton, P.D., Machado, R., Patel, D., Trembath, R.C., and Morrell, N.W.** (2002). Functional analysis of bone morphogenetic protein type II receptor mutations underlying primary pulmonary hypertension. Hum. Mol. Genet. **11,** 1517–1525.

**Sanchez, I., Hughes, R.T., Mayer, B.J., Yee, K., Woodgett, J.R., Avruch, J., Kyriakis, J.M., and Zon, L.I.** (1994). Role of SAPK/ERK kinase-1 in the stress-activated pathway regulating transcription factor c-Jun. Nature **372,** 794–798.

**Schneider, D.S., Hudson, K.L., Lin, T.Y., and Anderson, K.V.** (1991). Dominant and recessive mutations define functional domains of Toll, a transmembrane protein required for dorsal-ventral polarity in the Drosophila embryo. Genes Dev. **5,** 797–807.

**Schoof, H., Lenhard, M., Haecker, A., Mayer, K.F., Jurgens, G., and Laux, T.** (2000). The stem cell population of Arabidopsis shoot meristems is maintained by a regulatory loop between the CLAVATA and WUSCHEL genes. Cell **100,** 635–644.

**Shiu, S.H., and Bleecker, A.B.** (2001). Plant receptor-like kinase gene family: Diversity, function, and signaling. Sci. STKE **2001,** RE22.

**Sundaresan, V., Springer, P., Volpe, T., Haward, S., Jones, J.D., Dean, C., Ma, H., and Martienssen, R.** (1995). Patterns of gene action in plant development revealed by enhancer trap and gene trap transposable elements. Genes Dev. **9,** 1797–1810.

**Torii, K.U., and Clark, S.E.** (2000). Receptor-like kinases in plant development. In Advances in Botanical Research, M. Kries and J.C. Walker, eds (San Diego, CA: Academic Press), pp. 226–269.

**Torii, K.U., Mitsukawa, N., Oosumi, T., Matsuura, Y., Yokoyama, R., Whittier, R.F., and Komeda, Y.** (1996). The Arabidopsis ERECTA gene encodes a putative receptor protein kinase with extracellular leucine-rich repeats. Plant Cell **8,** 735–746.

**Trotochaud, A.E., Hao, T., Guang, W., Yang, Z., and Clark, S.E.** (1999). The CLAVATA1 receptor-like kinase requires CLAVATA3 for its assembly into a signaling complex that includes KAPP and a Rho-related protein. Plant Cell **11,** 393–405.

**Venglat, S.P., Dumonceaux, T., Rozwadowski, K., Parnell, L., Babi, V., Martienssen, R., Selvarag, G., and Datla, R.** (2002). The homeobox gene *BREVIPEDICELLUS* is a key regulator of inflorescence architecture in *Arabidopsis*. Proc. Natl. Acad. Sci. USA **99,** 4730–4735.

**Wang, G.L., et al.** (1998). Xa21D encodes a receptor-like molecule with a leucine-rich repeat domain that determines race-specific recognition and is subject to adaptive evolution. Plant Cell **10,** 765–779.

**Xiang, C., Han, P., Lutziger, I., Wang, K., and Oliver, D.J.** (1999). A mini binary vector series for plant transformation. Plant Mol. Biol. **40,** 711–717.

**Yokoyama, R., Takahashi, T., Kato, A., Torii, K.U., and Komeda, Y.** (1998). The Arabidopsis ERECTA gene is expressed in the shoot apical meristem and organ primordia. Plant J. **15,** 301–310.

**Zou, H., and Niswander, L.** (1996). Requirement for BMP signaling in interdigital apoptosis and scale formation. Science **272,** 738–741.